Gold Nanoparticle Strings Wrap up into Plasmonic Vesicles for Enhanced Photoacoustic Imaging

Yijing Liu[a], **Dr. Jie He**[a] **[co-first author]**, **Kuikun Yang**[a], **Dr. Chenglin Yi**[a], **Dr. Yi Liu**[a], **Dr. Liming Nie**[b], **Prof. Niveen M. Khashab**[c], **Dr. Xiaoyuan Chen**[b], and **Prof. Zhihong Nie**[a]

Xiaoyuan Chen: shawn.chen@nih.gov; Zhihong Nie: znie@umd.edu

[a]Department of Chemistry and Biochemistry, University of Maryland, College Park, Maryland, 20742

[b]Laboratory of Molecular Imaging and Nanomedicine (LOMIN), National Institute of Biomedical Imaging and Bioengineering (NIBIB), National Institutes of Health (USA)

[c]Smart Hybrid Materials (SHMs) Lab, Department of Chemical Sciences and Engineering Advanced, Membranes and Porous Materials Center, King Abdullah University of Science and Technology (KAUST), Thuwal 23955-6900, Kingdom of Saudi Arabia

Abstract

We report a stepwise self-assembly of hollow plasmonic vesicles containing strings of gold nanoparticles (NPs) in vesicular membranes. The formation of chain vesicles can be controlled by tuning the density of polymer ligands on the surface of gold NPs. The strong absorption of chain vesicles in the near-infrared (NIR) range led to a much higher efficiency in photoacoustic (PA) imaging than non-chain vesicles. The chain vesicles were further demonstrated for the encapsulation of drugs and NIR light-triggered release of payloads. This work not only offers a new platform for controlling the hierarchical self-assembly of NPs, but also demonstrates that the control over the spatial arrangement of NPs within the assemblies enables us to tailor the physical properties of the materials for better performance in biomedical applications.

Keywords

self-assembly; vesicles; photoacoustic imaging; block copolymer; gold nanoparticle string

---

Gold NPs (GNPs) have been extensively explored in nanomedicine, due to their unique size and intrinsic optical properties such as localized surface plasmon resonance and photothermal effect (i.e., the conversion of absorbed light to heat).[1] A GNP-based platform uniquely combines imaging (e.g., photothermal, photoacoustic (PA), and surface enhanced Raman scattering (SERS) imaging[2] and therapy in one system for cancer theranostics.[2a, 3] The organization of GNPs into defined nanostructures (e.g., clusters, chains, and vesicles) can further improve the performance of GNPs in nanomedicine.[4] For instance, one dimensional (1D) chains of GNPs show several orders of magnitude enhancement in the

---

electromagnetic field between NP gaps, thus giving rise to significantly improved SERS signal.[2e, 5] Moreover, the ability to tune the absorption of GNP chains enables their applications in photothermal cancer imaging and therapy using near-infrared (NIR) light source which has deep penetration in tissues.[6]

Recently, 3D vesicular assemblies of GNPs have been demonstrated as a new platform for effective cancer theranostics [2b, 2f, 6b, 7] The system not only serves as contrast agents for bioimaging, but also allows efficient loading of both hydrophobic and hydrophilic drugs.[2b, 7a, 7b, 8] To achieve optimal imaging and therapeutic outcomes, the interparticle spacing within these hybrid vesicles has to be carefully tuned to maximize their absorption in the NIR range. The red-shift of the plasmon peak from visible to NIR window is exponentially decayed with the ratio of interparticle distance to NP diameter.[7a] Although larger GNPs may give rise to stronger NIR absorption, small GNPs are usually more favorable with respect to their clearance from animal body.[4e] However, when the size of GNPs is small (<~15 nm), it becomes a challenge to tune the absorption of vesicular assemblies of GNPs to the NIR range.

Here we report the stepwise hierarchical self-assembly of block copolymer (BCP) tethered GNPs (BCP-GNPs) into hollow vesicles composed of GNP strings in the membrane (Figure 1). The assembly involves two critical steps: the organization of individual NPs into 1D strings and further wrapping of the strings into hollow vesicles (Figure 1b). The formation of chain vesicles rather than vesicles with uniform distribution of NPs in the membrane (referred to as non-chain vesicles) (Figure 1c) was achieved by tuning the grafting density (δ) of BCPs on the surfaces of GNPs. In this way, GNP strings with strong plasmonic coupling were obtained and used as buliding blocks for self-assembly of vesicles with strong absorption in the NIR window. We demonstrated the utilization of the hybrid vesicles as PA imaging probes and drug delivery vehicles. Compared with non-chain vesicles, the chain vesicles showed about eight-fold enhancement in the PA signal of *in vivo* imaging, while perserving their ability for the encapsulation and light triggered-release of therapeutic agents (Figure 1d).

Hexadecyltrimethylammonium bromide (CTAB) covered GNPs (13.0 ± 1.0 nm in diameter) were modified with thiol-terminated polystyrene-*b*-polyethylene oxide (PS-*b*-PEO) through an interfacial ligand exchange method we recently developed.[7a] The PS-*b*-PEO with a PS block of 31.6 K and a PEO block of 2 K was used throughout the work.[9] The δ was controlled in the range of 0.03 to 0.08 chain/nm^2 by varying the weight ratio of BCPs to GNPs during surface modification. The δ was estimated by thermal gravimetric analysis (TGA) (Figure S1 and Table S1). The BCP-GNPs were dispersed in tetrahydrofuran (THF) and the assembly of BCP-GNPs was triggered by the solvent exchange method (i.e., the dialysis of the solution against water).[7a, 8]

The formation of chain vesicle or non-chain vesicle was controlled by varying the δ of polymers on the GNP surfaces. At low δ (~0.03 chain/nm^2), the assembly process produced chain vesicles with a monolayer of GNP strings in the vesicular membranes (Figure 2a–c). When GNPs grafted with a higher δ (0.05 chain/nm^2) of BCPs were used, non-chain vesicles were formed and GNPs were relatively uniformly distributed in the vesicular

membranes (Figure 2d,e). The chain vesicle has an inner cavity that is separated from the environment through a thin membrane of GNP strings. The average diameter of the chain vesicles was 520 ± 170 nm, measured from dynamic light scattering (DLS) (Figure S2). This value was slightly smaller than that from TEM analysis, 673 ± 233 nm. This was possibly due to the collapse and flattening of vesicles under vacuum conditions. The GNP strings and networks can be clearly observed in vesicular membranes. TEM images further confirmed that the vesicles were hollow and made from a monolayer of GNP strings (Figure 2c and Figure S3a, S4b). The average separation distance between GNP strings within the chain vesicles was 12.3 ± 2.2 nm. The average number of GNPs in strings was about 6.2 per string. A close inspection of the chain vesicles indicates that the GNPs were in close contact with each other along the string; in some other cases, the GNPs were even fused together (inset of Figure 2c). The fusion of adjacent GNPs can be explained by a cold welding mechanism, where gold atoms can diffuse by means of surface diffusion.[10] Moreover, the attractive hydrophobic interaction and van der Waals interaction may also facilitate the fusion of adjacent GNPs.

The average interparticle distance between GNPs within each string is 0.8 ± 0.1 nm, which is much smaller than that of 9.0 ± 1.5 nm between GNPs in non-chain vesicles. The small interparticle distance within each string in chain vesicles leads to strong NIR absorption caused by the strong coupling between adjacent GNPs.[7a, 11] Compared to non-chain vesicles made from the same sized GNPs, chain vesicles have two distinct peaks located at 545 nm and 780 nm, while the non-chain vesicles only have one absorption peak between 590 nm to 620 nm (Figure 2f).

We systematically investigated the formation mechanism of chain vesicles using UV-vis spectroscopy and TEM imaging. Water was added stepwise (at an interval of 1 vol.%) into a solution of BCP-GNPs in THF to trigger the self-assembly. At 5 vol.% water, both TEM image and UV-vis spectra reveal that most BCP-GNPs remained as individual NPs (Figure 3a,b). With the increase of water content to ~10 vol.%, 1D strings of GNPs were formed, as indicated by TEM images and the appearance of a new peak at 607 nm in UV-vis (Figure 3a,c). At 20 vol.% and 100 vol.% water content, all the 1D strings rolled into chain vesicles (Figure 3d). This process was accompanied with the further red-shift of plasmon peak. This result suggests a novel two-step hierarchical self-assembly process: the formation of NP strings from individual NPs and subsequent assembly of NP strings into vesicles.

The competition in the formation of chain or non-chain vesicles can be explained as follows: At low polymer δ, as a result of the strong van der Waals force between a pair of very closely associated GNPs, the segments of BCP chains are squeezed out of the gap between NP pairs, leading to a higher polymer density around the center than both poles of NP pairs (Figure 3e). This results in strong three-body repulsive forces at the center of NP pairs.[12] The repulsion at the center and van der Waals attraction at both poles induce the formation of 1D GNP strings at the early stage of chain vesicle formation (Figure 3e). This is consistent with the fact that the separation distance between strings (~12 nm) in chain vesicles is larger than that between GNP pairs in each string (~0.8 nm). Unlike most of 1D colloidal assemblies reported previously,[5c, 5d, 13] the electrostatic repulsion is not the dominant repulsive force in the process of string formation, largely due to the low dielectric

constant (12.59) of the mixed solvent (10% of water in THF).[14] This is envidenced by our controlled experiment: the formation of chain vesicles was not prone to the presence of electrolytes (0–500 mM NaCl). Upon further addition of water, the instability of GNP strings leads to their association into enclosed vesicles in order to minimize the interfacial tension (Figure S5). In contrast, at high δ, the GNPs are separated fairly far in the NP pairs, which dramatically weaken the van der Waals attractions between GNPs. The steric repulsions are mainly balanced by attractive hydrophobic interactions. To maximize hydrophobic interactions, individual NPs approach from the sides of clusters to form 2D thin films and eventually non-chain vesicles (Figures S5 and S7).

The linear organization of GNPs in chain vesicles result in a strong NIR absorption of the assemblies, due to the strong coupling between GNPs in the strings, which is preferred for *in vivo* biomedical applications. GNPs absorb light and emit an acoustic wave that can be detected by a ultrasonic detector, thus enabling the visualization of biological tissues, that is, the so-called photoacoustic (PA) imaging.[15] PA imaging is an emerging biomedical modality with deep imaging depth and high spatial resolution.[16] The chain vesicles and non-chain vesicles were demonstrated for PA imaging *in vivo*. Two types of vesicles containing the same amount of gold materials (50 μg) were subcutaneously injected into the flank of nude mice. The injected area was irradiated with a pulsed NIR laser (780 nm with power density of 60 mW/cm^2) for equal amount of time. The chain vesicle group showed 8.0-fold enhancement in the PA signal, compared to the control group without the injection of PA contrast agents (Figure 4a,b). In contrast, the non-chain vesicle group showed only 1.1 times enhancement of PA signal (Figure 4c,d). The inner cavity of the hybrid vesicles can load hydrophilic drugs, which makes the vesicles an ideal platform for drug delivery.[2f] We demonstrated that GNP vesicles can be used as drug delivery vehicles and the release of payloads can be remotely triggered by NIR light. Rhodamine B (RhB) was encapsulated in the chain vesicles as a model drug during the self-assembly of vesicles. After the removal of free dye molecules, the RhB loaded chain vesicles were exposed to NIR light (780 nm pulsed laser, 60 mW/cm^2) at a time interval of 10 min. The fluorescence emission at 560 nm in the solution was measured to monitor the release of RhB and it almost linearly increased with irradiation time (Figure S11). Without laser irradiation, the fluorescence intensity in the solution only slightly increased for about 13% of the laser irradiation group. An examination of vesicles before and after light illumination by SEM shows that NIR light induced the collapse of the integrity of the chain vesicles (Figure S12). In addition, our vesicles are stable under physiological conditions and the adjusted physical conditions (i.e. ionic strength and pH) (Figure S13). These results demonstrate the potential of chain vesicles in bioimaging and drug delivery.

In summary, we have developed a new strategy for the fabrication of GNP chain vesicles with strong NIR absorption as drug delivery vehicles and PA imaging contrast agents. The chain vesicles were assembled from BCP-GNPs through a new stepwise hierarchical self-assembly mechnism, in which the competition between attractive and repulsive forces is govened by the δ of polymer ligands on GNPs. The strong NIR absorption of the chain vesicles arising from the strong plasmon coupling between GNPs within 1D strings results in higher efficiency of chain vesicles in PA imaging than non-chain vesicles. This study not

only demonstrates that the properties of hybrid vesicles can be improved by engeering the arrangement of the NPs within the assemblies, but also provides us the fundamental understanding of stepwise self-assembly of colloidal NPs for the fabracation of more complex nanostructures.

Supplementary Material

Refer to Web version on PubMed Central for supplementary material.

Acknowledgments

References

1. a) Arvizo RR, Bhattacharyya S, Kudgus RA, Giri K, Bhattacharya R, Mukherjee P. Chem Soc Rev. 2012; 41:2943–2970. [PubMed: 22388295] b) Doane TL, Burda C. Chem Soc Rev. 2012; 41:2885–2911. [PubMed: 22286540]

2. a) Nie Z, Fava D, Kumacheva E, Zou S, Walker GC, Rubinstein M. Nat Mater. 2007; 6:609–614. [PubMed: 17618291] b) He J, Wei Z, Wang L, Tomova Z, Babu T, Wang C, Han X, Fourkas JT, Nie Z. Angew Chem Int Ed. 2013; 52:2463–2468.

3. a) Zhang Z, Wang J, Chen C. Theranostics. 2013; 3:223–238. [PubMed: 23471510] b) Song J, Zhou J, Duan H. J Am Chem Soc. 2012; 134:13458–13469. [PubMed: 22831389] c) Liu Y, Liu Y, Yin JJ, Nie Z. Macromole Rapid Commun. 2015; 36:711–725.d) Austin LA, Kang B, El-Sayed MA. Nano Today. 201510.1016/j.nantod.2015.07.005e) Hu H, Duan H, Yang JKW, Shen ZX. ACS Nano. 2012; 6:10147–10155. [PubMed: 23072661] f) Lin J, Wang S, Huang P, Wang Z, Chen S, Niu G, Li W, He J, Cui D, Lu G, Chen X, Nie Z. ACS Nano. 2013; 7:5320–5329. [PubMed: 23721576]

4. Dreaden EC, Alkilany AM, Huang X, Murphy CJ, El-Sayed MA. Chem Soc Rev. 2012; 41:2740–2779. [PubMed: 22109657]

5. a) Wang L, Zhu Y, Xu L, Chen W, Kuang H, Liu L, Agarwal A, Xu C, Kotov NA. Angew Chem Int Ed. 2010; 49:5472–5475.b) Klinkova A, Thérien-Aubin H, Ahmed A, Nykypanchuk D, Choueiri RM, Gagnon B, Muntyanu A, Gang O, Walker GC, Kumacheva E. Nano Lett. 2014; 14:6314–6321. [PubMed: 25275879] c) Jaganathan H, Ivanisevic A. J Mater Chem. 2011; 21:939–943.d) Liu K, Nie Z, Zhao N, Li W, Rubinstein M, Kumacheva E. Science. 2010; 329:197–200. [PubMed: 20616274] e) Chou LYT, Zagorovsky K, Chan WCW. Nat Nanotechnol. 2014; 9:148–155. [PubMed: 24463361] f) Liu Y, Yin JJ, Nie Z. Nano Res. 2014; 7:1719–1730.

6. a) Xi C, Facal PM, Xia H, Wang D. Soft Matter. 2015; 11:4562–4571. [PubMed: 25994925] b) Chen G, Wang Y, Yang M, Xu J, Goh SJ, Pan M, Chen H. J Am Chem Soc. 2010; 132:3644–3645. [PubMed: 20196540] c) Xia H, Su G, Wang D. Angew Chem Int Ed. 2013; 52:3726–3730.d) Zhang H, Wang D. Angew Chem Int Ed. 2008; 120:4048–4051.e) Choueiri RM, Klinkova A, Therien-Aubin H, Rubinstein M, Kumacheva E. J Am Chem Soc. 2013; 135:10262–10265. [PubMed: 23806016]

7. a) Loo C, Lowery A, Halas N, West J, Drezek R. Nano Lett. 2005; 5:709–711. [PubMed: 15826113] b) Huang P, Lin J, Li W, Rong P, Wang Z, Wang S, Wang X, Sun X, Aronova M, Niu G, Leapman RD, Nie Z, Chen X. Angew Chem Int Ed. 2013; 52:13958–13964.

8. a) He J, Huang X, Li YC, Liu Y, Babu T, Aronova MA, Wang S, Lu Z, Chen X, Nie Z. J Am Chem Soc. 2013; 135:7974–7984. [PubMed: 23642094] b) Song J, Cheng L, Liu A, Yin J, Kuang M, Duan H. J Am Chem Soc. 2011; 133:10760–10763. [PubMed: 21699155]

9. Liu Y, Li Y, He J, Duelge KJ, Lu Z, Nie Z. J Am Chem Soc. 2014; 136:2602–2610. [PubMed: 24447129]

10. He J, Liu Y, Babu T, Wei Z, Nie Z. J Am Chem Soc. 2012; 134:11342–11345. [PubMed: 22746265]

11. Lu Y, Huang JY, Wang C, Sun S, Lou J. Nat Nanotechnol. 2010; 5:218–224. [PubMed: 20154688]

12. a) Jain PK, Huang W, El-Sayed MA. Nano Lett. 2007; 7:2080–2088.b) Reinhard BM, Siu M, Agarwal H, Alivisatos AP, Liphardt J. Nano Lett. 2005; 5:2246–2252. [PubMed: 16277462]

13. Rubinstein, M.; Colby, RH. Polymer physics. Oxford University Press; Oxford; New York: 2003.

14. Yang M, Chen G, Zhao Y, Silber G, Wang Y, Xing S, Han Y, Chen H. Phy Chem Chem Phy. 2010; 12:11850–11860.

15. Critchfield FE, Gibson JA, Hall JL. J Am Chem Soc. 1953; 75:6044–6045.

16. Xu M, Wang LV. Rev Sci Instrum. 2006; 77:041101.

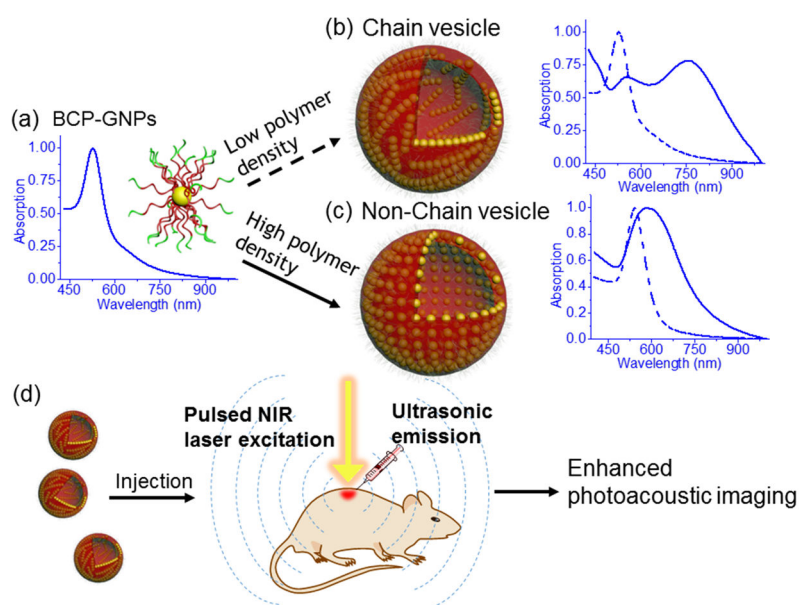17. Li W, Chen X. Nanomedicine. 2015; 10:299–320. [PubMed: 25600972]

Figure 1.
(a–c) Schematic illustration of the self-assembly of BCP-GNPs into chain vesicles and non-chain vesicles and (d) the enhanced PA imaging with chain vesicles.
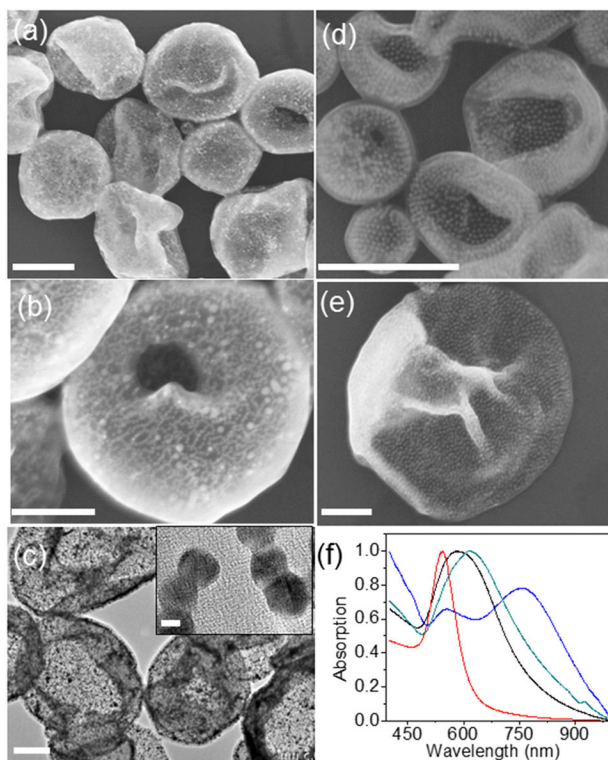
Figure 2.
(a–c) Representative SEM (a,b) and TEM (c) images of chain-vesicles made from BCP-GNPs comprising 13 nm GNPs as cores. The inset in (c) shows some GNPs in the strings within chain vesicles are fused together. (d,e) Representative SEM images of non-chain vesicles made from BCP-GNPs comprising 13 nm GNP cores. (f) The UV-vis spectra of individual GNPs (red), non-chain vesicles (green and black), and chain vesicle (blue). The chain vesicles and two non-chain vesicles were prepared by using BCP-GNPs with δ of 0.03, 0.05, and0.08 chain/nm^2, respectively. Scale bars: 500 nm in (a) and (d), 250 nm in (b) and (e), 200 nm in (c) and 5 nm in the inset of (c).
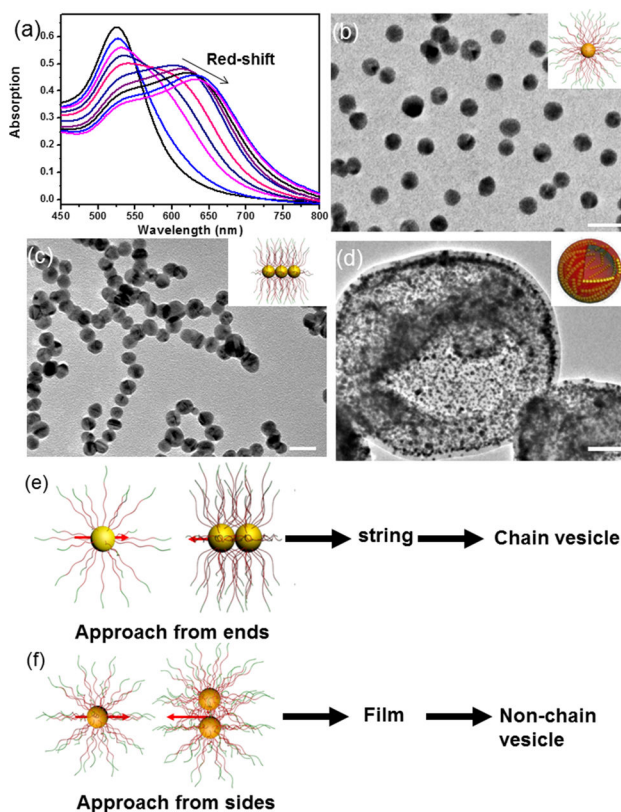
Figure 3.
The mechanism and kinetics of the self-assembly of BCP-GNPs with 13 nm cores. (a) UV-vis spectra of BCP-GNPs with 13 nm cores at different water concentrations. (b–d) Representative TEM images of assemblies obtained at 5, 10 and 100 vol.% of water in water/THF mixture. Scale bars: 20 nm in (b) and (c), 100 nm in (d). (e, f) Schematic illustration of the formation mechanism of chain vesicles (e) and non-chain vesicles (f).
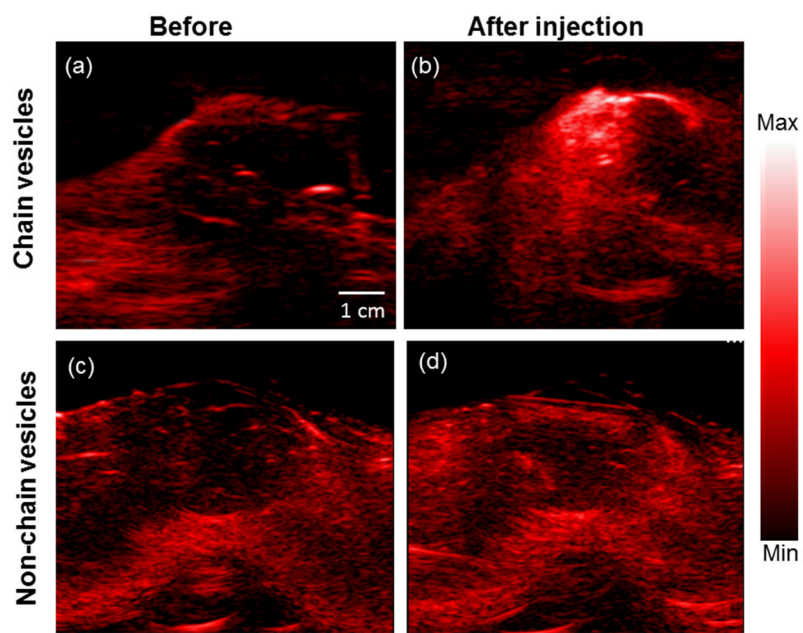
Figure 4.
In vivo 2D PA imaging of mouse tissue before and after the injection of chain vesicles (a, b) and none chain vesicle (c, d).